

## New Compact Circular Ring Microstrip Patch Antennas

Mohamed A. Abdelaal\* and Hussein Hamed Mahmoud Ghouz

**Abstract**—In this paper, three different compact circular-ring microstrip patch antenna structures have been proposed. These antennas have been analyzed, investigated and optimized using the CST-MW-simulator. The proposed designs are mainly based on the concept of patch shape reconfiguration while its overall dimensions are kept constant. The objective is to design dual and/or triple broadband antennas resonate within the fourth generation band (4G). The presented antennas are simulated and fabricated on cheaper and lossy FR-4 substrate, and their parameters are measured and compared. The obtained results show that the proposed antenna structures resonate within the 4G frequency band. The operating bandwidths have been varied between 270.0 MHz and 1000.0 MHz (about 4% up to 7% of center frequency). In addition, maximum VSWR value of less than 1.5 has been achieved. The obtained results verify the validity and the benefits of reconfiguring the patch shape. Finally, good agreement has been obtained between simulated and measured parameters.

### 1. INTRODUCTION

Planar antenna configurations have numerous benefits in wireless communications and radar systems applications. This is due to their small size, low cost, less weight, and easy fabrication. In particular, microstrip circuits have excellent compatibility with the typical manufacturing process of planar MMIC circuits. A huge number of studies have been done in the area of planar antennas. This includes different shapes and structures, for example, rectangular patch having dual broad band characteristic was reported in [1]. An antenna system composed of a combination of several transmission lines and multi ports has been proposed in [2]. Such antenna structure operates as dual-band WLAN in the frequency band of 2.4–2.5 GHz and 5.15–5.825 GHz. Another trend is to use a parasitic patch and driven patch was presented in [3]. The two patches together formed an antenna that operates at dual-band frequencies with enhanced bandwidths. A new patch has a stair case shape with partial ground was reported in [4]. The partial ground and the compact patch have an UWB operation in the frequency range of 3.1 GHz to 10.6 GHz. An inset feed E-shape patch antenna was proposed, optimized and reported in [5]. E-shape with the selected dimensions had an effect of forcing the resonance frequency to be from 2.40–2.52 GHz with bandwidth of 121.9 MHz. A unified approach was presented in [6] for achieving both broad band and dual-band operation by offsetting the antennas feed line. These antennas have a folded slot patch. In [7] a novel monopole patch shape was proposed as an UWB (3.1–10.6 GHz). This patch contains different shapes of curved slots, an external rectangular hollow resonator and a partial ground. A different L-probe fed patch antenna was presented in [8]. It resonates at frequency range from 2.3 to 2.7 GHz. In [9] a critical overview of possible solutions for dual-frequency patch antennas was presented, and future perspectives were outlined. A planar quasi-monopole antenna with a simple structure and low-profile was proposed in [10]. Such antenna is usually used for UWB applications. Finally in [11] a compact dual-band microstrip patch antenna with U-shape slot was discussed. The antenna compactness and its operating frequencies are suitable for MIMO 4G LTE and WLAN. In this

---

*Received 16 December 2013, Accepted 9 January 2014, Scheduled 16 January 2014*

\* Corresponding author: Mohamed A. Abdelaal (mabdelaal@ieee.org).

The authors are with the Department of Electronics and Communications Engineering, Arab Academy for Science, Technology and Maritime Transport (AASTMT), Cairo, Egypt.

paper three proposed compact planar microstrip patch antennas are analyzed, investigated, optimized, fabricated, measured and presented. The proposed antennas structures resonate within the 4G band that has widely applications in wireless communication systems. Section 2 presents a detailed description of a conventional circular patch antenna and its proposed versions. The procedures to achieve the proposed designs are also completely described in this section. In Section 3 the key simulation parameters of the proposed antennas are discussed. Simulation of the patch current distribution is also investigated and analyzed. Fabrication of the three proposed antenna configurations and their measured parameters are presented in Section 4. Such antennas resonate at dual and/or triple frequencies with a symmetric and wide bandwidth about the required resonance frequency. Finally, Section 5 concludes the paper's contribution.

## 2. DESCRIPTION AND DESIGN OF THE PROPOSED CIRCULAR RING PATCH

A Conventional Circular Patch (CCP) antenna configuration with radius ( $R_1$ ) is illustrated in Figure 1(a). It is mounted on a single FR-4 substrate ( $\epsilon_r = 4.3$ , 1.6 mm height, and tangential loss of 0.02). The conductor thickness is assumed to be 0.035 mm and the transmission line feed is 50 Ohm of length 15 mm. The antennas dimensions and description are listed in Table 1. This assumed antenna has been selected with these dimensions in order to be compact. Then, it is modified and optimized to operate in the 4G frequency band. Such antenna has been used as reference one to be compared with the proposed antennas. A procedure composed of three steps is done on CCP configuration so that the antennas meet the 4G frequency band. This procedure has been conducted through the simulations carried out using CST Microwave Studio Simulator [12], and it is summarized as follows. First, convert the CCP antenna to a Circular Ring Patch (CRP) antenna with inner radius ( $R_2$ ) as shown in Figure 1(b). The value of ( $R_2$ ) has been selected after a complete parametric study of several inner radius values. The second step is to add an inner circular patch inside the ring patch with radius ( $r$ ). The value of ( $r$ ) has been selected after conducting a detailed parametric of radius values. In addition, the radius value of the inner resonator has been selected so that the feeder can be easily extended inside the patch. Finally, the feeder is extended inside the patch with value of ( $E_x$ ). A parametric analysis was carried out to select the optimum values of the feeder extension length values. The selected values of the feeder extension length are found to be 2.5 mm and 3.5 mm. These antennas are referred to as Circular Ring Patch with Inner Resonator and Extended Feeder (CRPIR\_EF\_2.5 and CRPIR\_EF\_3.5) respectively as illustrated in Figure 1(c) The selected configurations from the previous study are CRPIR\_EF\_2.5 and CRPIR\_EF\_3.5. These antennas are dual band antennas as their results are presented in the next section. An extra resonance frequency is needed in order to make the antenna operates at triple frequencies. The antenna configuration must be modified to achieve such goal. First, the feeder is extended to the end of the ring and the extra inner resonator radius must be increased in order to appear and not submerged with the feeder, so its radius is doubled (i.e., the radius value is 3 mm). Second, an outer rectangular resonator is added. Its length ( $L_r$ ), width ( $W_r$ ) and separation between the outer rectangular resonator and the circular ring patch ( $X_r$ ). The dimensions and position

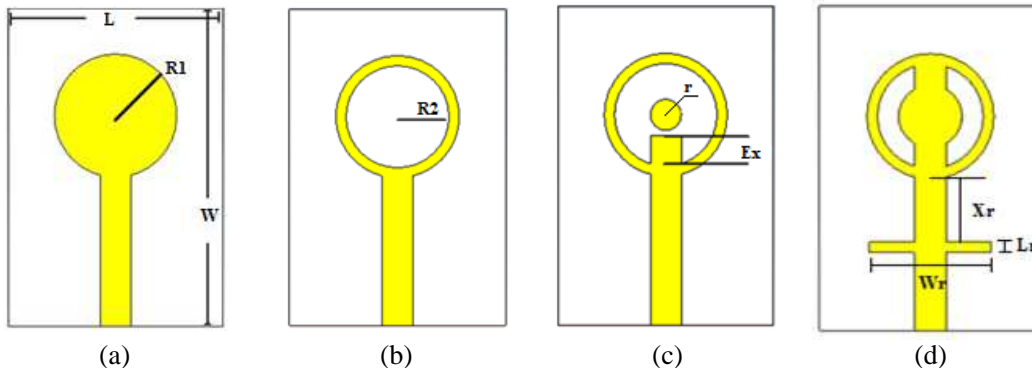


**Figure 1.** Antenna configuration of CCP, CRP CRPIR\_EF\_2.5 and CRPIER\_EF\_10.0 respectively.

of the external resonator are optimized. This proposed configuration is referred to as Circular Ring Patch with Inner and External Resonator and Extended Feeder by 10.0 mm (CRPIER\_EF\_10.0) antenna and it is shown in Figure 1(d).

Table 1 shows the parameter names and their description. Such parameters are used to design the selected antenna configurations. The feeder extension ( $E_x$ ) controls the values of the dual frequencies, where as its value increases, the lower frequency becomes lower while the upper frequency shifts to a higher band. The external rectangular resonator length and width control the resonance frequencies values and depth. Finally, the location of the external rectangular resonator ( $X_r$ ) is very important parameter. It is responsible for creating another resonance frequency such that the antenna resonates at triple frequencies. As the value of ( $X_r$ ) decrease the operating frequencies tend to be only dual, also the lower frequency is shifted up while the upper frequency becomes lower. When the value of ( $X_r$ ) is higher than the optimum value, the triple resonance frequencies are shifted lower but with rapid decrease of dB depth until the middle frequency vanishes.

**Table 1.** Antennas parameters description and values.

Parameter Name	Parameter Description	Parameter value (mm)
$L$	Substrate length	31
$W$	Substrate width	21
$R_1$	Circular radius or external ring radius	6
$R_2$	Internal ring radius	5
$r$	Internal circular resonator radius	1.5 (for CRPIR_EF_2.5, 3.5) 3 (for CRPIER_EF_10.0)
$E_x$	Feeder extension inside the ring resonator	2.5 (for CRPIR_EF_2.5) 3.5 (for CRPIR_EF_3.5) 10 (for CRPIER_EF_10.0)
$L_r$	External rectangular resonator length	1 (optimum)
$W_r$	External rectangular resonator width	11.5 (optimum)
$X_r$	Spacing between external rectangular resonator and external ring edge	6 (optimum)

### 3. RESULTS AND DISCUSSIONS

It is clear from Figure 2 that CCP antenna resonates at higher frequency band of about 11 to 13 GHz. The 4G frequency band is much lower than CCP frequencies so it is needed to bring them to the requested band (Wi-Fi, WiMAX and LTE). The selected value of ( $R_2$ ) of the ring patch (CRP) is 5 mm. This value permits large space so that an extra internal resonator can be added. In Figure 2 CRP (with  $R_2 = 5$  mm) antenna resonates at 14 GHz with bandwidth of 900 MHz. The operating frequency is in the Ku-band and needs to be brought to the 4G band. Figure 3(a) compares the CCP to the circular patch with internal circular resonator and no extension in feed line (CRPIR\_EF\_0.0). It is also clear from Figure 3(a) that the feed line needs to be extended so that the resonance frequencies can meet the desired frequency band. Figure 3(b) demonstrates that when the feed line is extended, the resonance frequencies become close to the desired frequency band. The selected values of extension are 2.5 and 3.5 mm. Also Figure 3(b) demonstrates that CRPIR\_EF\_2.5 antenna resonates at 8.96 and 12.703 GHz with bandwidth of 350 and 560 MHz respectively. The other microstrip configuration, CRPIR\_EF\_3.5 antenna resonates at 7.52 and 14.15 GHz with bandwidth of 330 and 1000 MHz respectively. As a summary, the two selected antenna configurations are CRPIR\_EF\_2.5 and CRPIR\_EF\_3.5 because their resonance frequencies are within the 4G band so that they can be used for different applications. An extra resonance frequency is needed so that the antenna can operate at triple frequencies. The antenna configuration is modified (as discussed in the previous section) to achieve such goal. Figure 4 illustrates

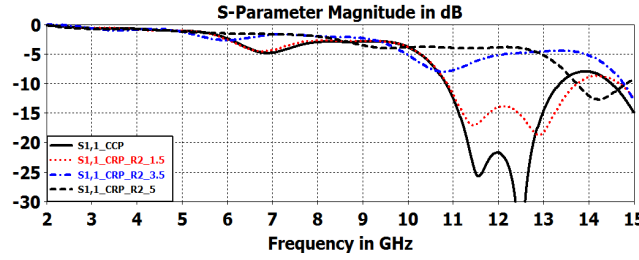


Figure 2.  $|S_{11}|$  of CCP and CRP (with different  $R_2$  values) antennas.

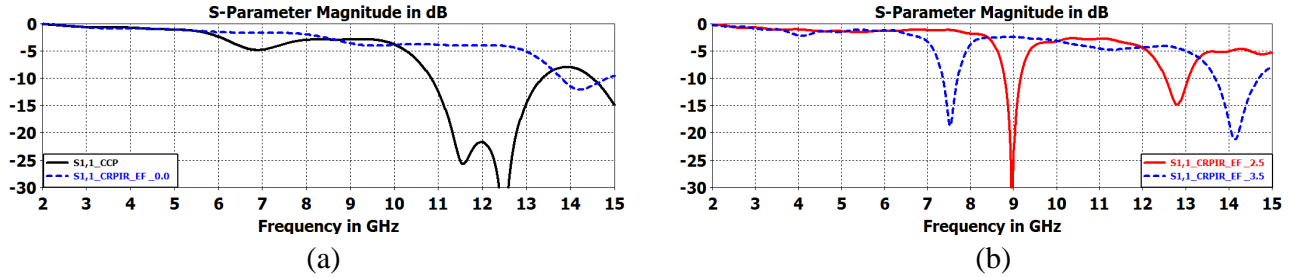


Figure 3. (a)  $|S_{11}|$  of CCP and CRPIR\_EF\_0.0 antennas. (b)  $|S_{11}|$  of CRPIR\_EF\_2.5 and CRPIR\_EF\_3.5 antennas.

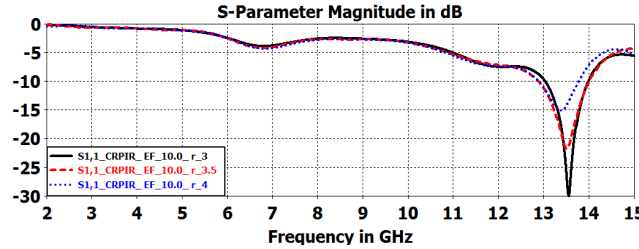
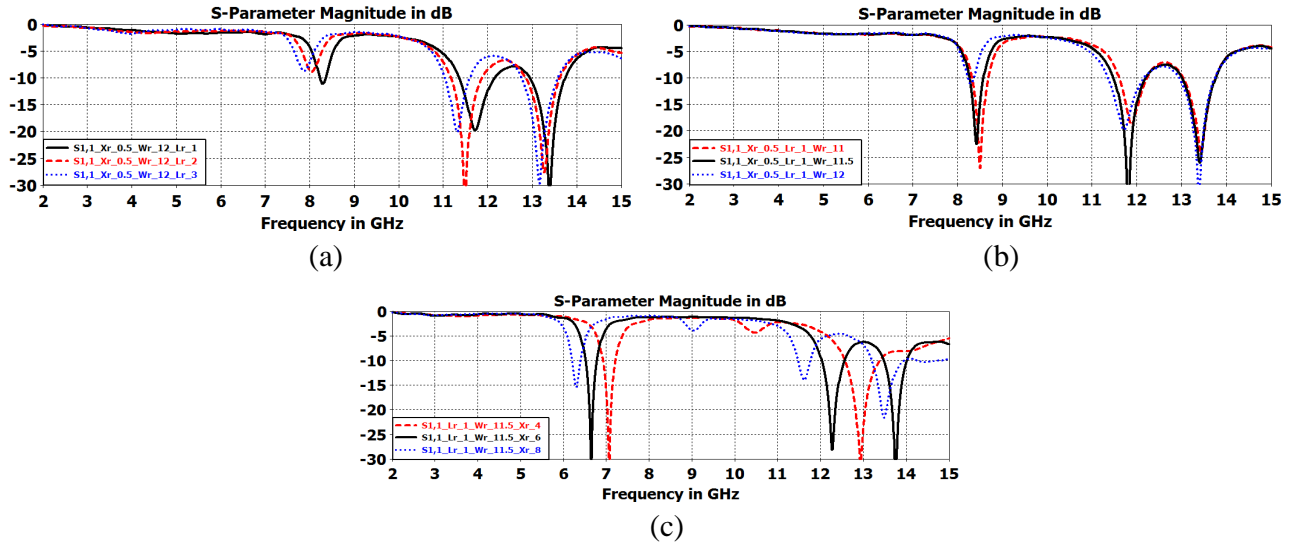


Figure 4.  $|S_{11}|$  of CRPIR\_EF\_10.0 with different ( $r$ ) values antenna.

a parametric study of the internal resonator radius value ( $r$ ). This is done after the feed line is fully extended. The radius value controls the depth of the single resonance frequency. The selected value is 3 mm. An external resonator is then added to create new dual frequencies. The external rectangular resonator parameters are ( $L_r$ ), ( $W_r$ ) and ( $X_r$ ) They are optimized based on a study of their effect on the resonance frequencies as shown in Figure 5(a) through (c). As a result of such study the optimum selected values of ( $L_r$ ), ( $W_r$ ) and ( $X_r$ ) are 1 mm, 11.5 mm and 6.0 mm respectively. The antenna configuration of such optimum selected values is shown in Figure 5(c) with black color. Also this figure demonstrates that CRPIER\_EF\_10.0 antenna resonates at 6.68, 12.37 and 13.75 GHz with bandwidth of 270, 460 and 480 MHz respectively. This antennas configuration is also selected (i.e., three configurations are selected in this research).

To investigate the impact of shape reconfiguration concept on the patch resonances, the current distribution should be studied and compared to the conventional patch (CCP). The current distribution of CCP, CRP, CRPIR\_EF\_3.5 and CRPIER\_EF\_10.0 antennas are presented in Figure 6(a) through (d). Same scale is used for all presented current distributions. Figure 6(a) illustrates the current distribution of CCP antenna at 12 GHz. It is clear that the current is concentrated mainly on the circular disk and feed line edges. This current is considered as a reference to the other circular patch configurations. When the circular disk patch is converted to a circular ring (CRP), the resonating metallic area becomes very small affecting the current distribution as shown in Figure 6(b). The current distribution is concentrated on the inner and outer edges of the circular ring. The resonance frequency of the ring patch is moved to



**Figure 5.** (a)  $|S_{11}|$  of CRPIER\_EF\_10.0 antenna with different external resonator lengths. (b)  $|S_{11}|$  of CRPIER\_EF\_10.0 antenna with different external resonator widths. (c)  $|S_{11}|$  of CRPIER\_EF\_10.0 antenna with different external resonator locations.

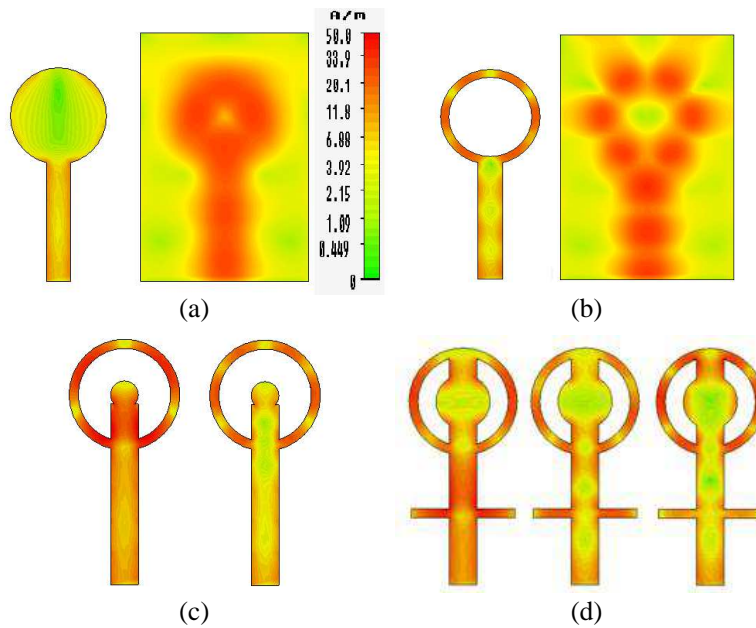


**Figure 6.** (a) Current distribution of CCP antenna. (b) Current distribution of CRP antenna. (c) Current distribution of CRPIER\_EF\_3.5. (d) Current distribution of CRPIER\_EF\_10.0.

14.216 GHz instead of 12 GHz. In Figure 6(c) the current distribution of CRPIER\_EF\_3.5 is concentrated on the ring surface, on the internal circular resonator, and on the extended feeder. The metallic resonating area is increased so the resonance frequency value is changed. The resonance frequencies become 7.52 and 14.15 GHz. The modified version of CRPIER\_EF\_3.5 antenna is CRPIER\_EF\_10.0 antenna. Its current distribution is shown in Figure 6(d). It is concentrated on the ring surface, on the external edges of the internal circular resonator, on the rectangular resonator surface, and on the feed line. The overall metallic resonating area is completely enlarged if compared to the CCP antenna, so the resonance frequencies are changed to be 6.68, 12.37 and 13.75 GHz. Three microstrip

patch antenna structures have been selected. These antennas are CRPIR\_EF\_2.5, CRPIR\_EF\_3.5 and CRPIER\_EF\_10.0. A fine simulation is done to find the selected antennas parameters. These parameters include resonance frequencies, bandwidths gains, maximum radiation efficiency, and VSWR. Such parameters are shown in Table 2. The radiation patterns of the proposed antennas are shown in Figure 7 through Figure 9.

**Table 2.** Proposed antennas parameters.

	CRPIR_EF_2.5	CRPIR_EF_3.5	CRPIER_EF_10.0
Resonance Frequency (GHz)	8.96	7.52	6.68
	12.8	14.15	12.37 13.75
Bandwidth (MHz)	350	330	270
	560	1000	460 480
Max. Antenna Gain (dB)	3.53	8.71	4.15
			3.25 3.35
Min. Antenna Gain (dB)	3.15	8.15	3.15
Max. Total Radiation Efficiency	55%	55%	59%
			60% 62%
Max. VSWR	1.04	1.26	1.04
	1.50	1.1	1.10 1.03

It is clear from Figure 7 that at frequency of 8.96 GHz the antenna is directive and has a large beam width; however at 12.8 GHz, the pattern becomes less directive which leads to decreasing the beam width. The back lobes at dual frequencies have a significant value that can be used for transmission or reception. The radiation pattern of CRPIR\_EF\_2.5 antennas at 12.8 GHz becomes more directive in the  $H$ -plane, in  $E$ -plane the beam width increases and the back lobes becomes more effective on the pattern. As shown in Figure 8 CRPIR\_EF\_3.5 antenna is directive in both planes and has a beam width smaller than that of CRPIR\_EF\_2.5 at frequency of 7.52 GHz. Also the back lobes have a smaller value that can be also used for transmission or reception. At frequency of 14.15 GHz the pattern beam width becomes very large and the antenna back lobes size increases, thus the antenna acts as a semi-Omni directional in both planes. Figure 9 demonstrates that CRPIER\_EF\_10.0 antenna is directive in both planes at 6.68 GHz while it is less in directivity at 12.37 GHz. At 13.75 GHz  $E$ -plane pattern is directive but with an inclination angle, however, the  $H$ -plane has no inclination angle and the pattern is completely directive. The back lobes can be also used for transmission or reception.

#### 4. FABRICATION AND MEASUREMENTS

The selected antenna configurations are fabricated and tested. They are measured and compared to the simulation results. Layout generation can be conducted using Computer Added Drawing (CAD) software for preparing the mask. Once the mask is printed on a transparent sheet; the patch can be fabricated using conventional photolithography process. The name and the description of each configuration to be fabricated from the three proposed configurations are listed as: Config.1: Circular Ring Patch with Inner Resonator and Extended Feeder by 2.5 mm (CRPIR\_EF\_2.5), Config.2: Circular Ring Patch with Inner Resonator and Extended Feeder by 3.5 mm (CRPIR\_EF\_3.5), and Config.3: Circular Ring Patch with Inner and External Resonator and Extended Feeder by 10.0 mm (CRPIER\_EF\_10.0). These proposed configurations are measured and compared to the simulation

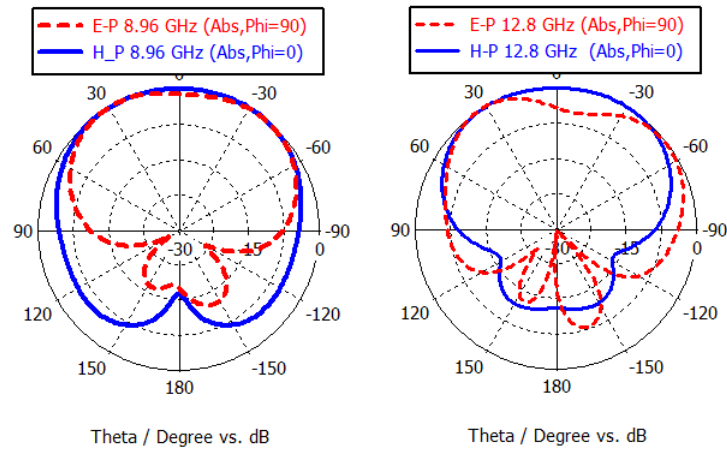


Figure 7. Radiation pattern of CRPIR\_EF\_2.5 antenna.

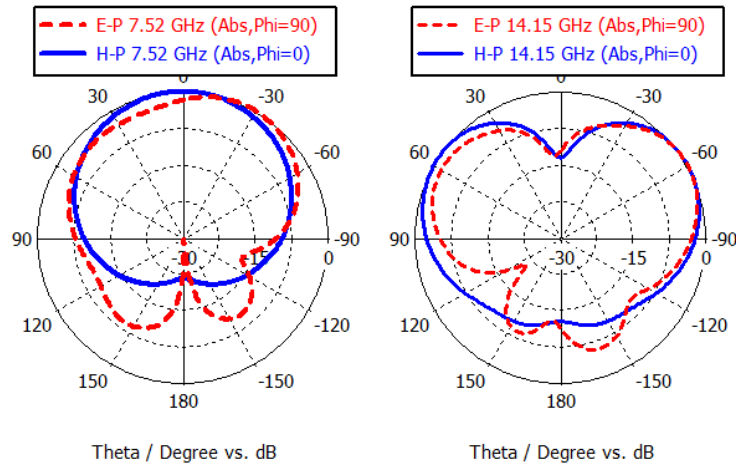


Figure 8. Radiation pattern of CRPIR\_EF\_3.5 antenna.

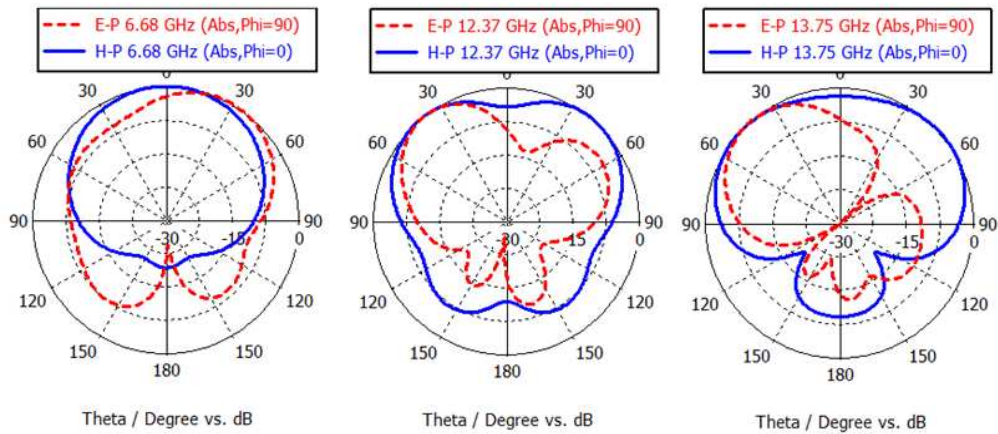
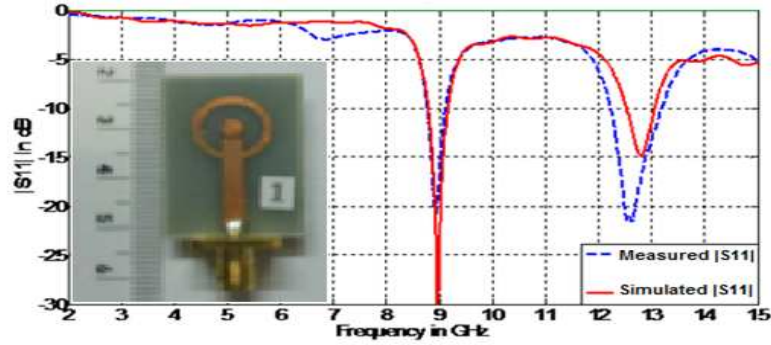
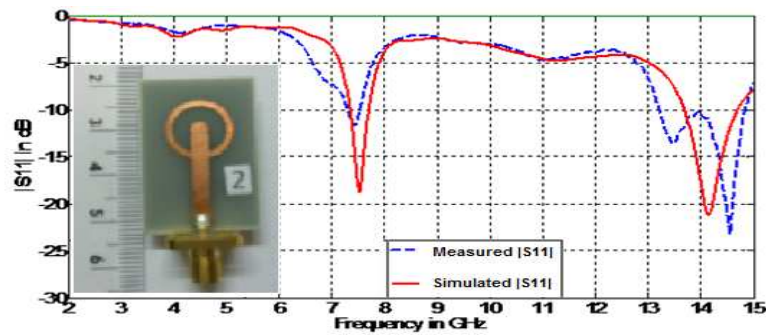


Figure 9. Radiation pattern CRPIER\_EF\_10.0 antenna.



**Figure 10.** Measured and simulated  $|S_{11}|$  of antenna configuration number 1 (Config.1).



**Figure 11.** Measured and simulated  $|S_{11}|$  of antenna configuration number 2 (Config.2).

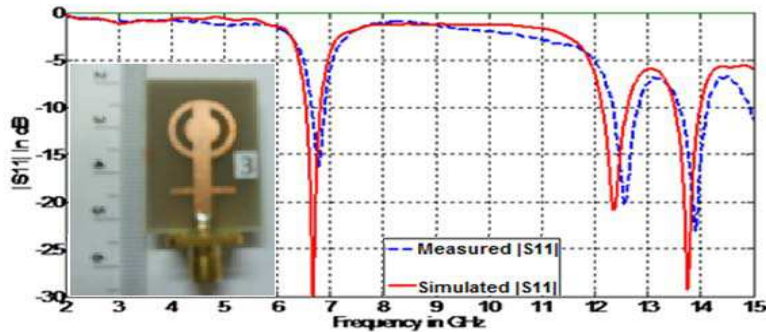


**Figure 12.** Measured and simulated  $|S_{11}|$  of antenna configuration number 3 (Config.3).

results. The fabricated antennas (photos) and their measured  $s$ -parameters are presented in Figure 10 through Figure 12 as well as the simulation results.

It is clear from Figure 10 that the fabricated antenna (Config.1) resonates at dual frequencies. The lower frequency is about 9 GHz which is identical to the simulated results. The higher resonance center frequency is not the same, it is slightly shifted, however, the bandwidth of the measured antenna is larger than the simulations. The second antenna configuration results are presented in Figure 11. This fabricated antenna (Config.2) is broadband dual frequencies antenna. The lower frequency is about 7.5 GHz which is so close to the simulated results but with difference in dB depth. The higher resonance frequency is not congruent with the simulated one, however, the bandwidth covered is larger. Finally, Figure 12 illustrates the  $s$ -parameters of the third fabricated antenna structure (Config.3). This antenna resonates at broadband-triple frequencies. The measured resonance frequencies and their bands are in good agreement with the corresponding simulated values.

## 5. CONCLUSIONS

The presented study introduces a new concept of reconfigurable antenna patch where the outer patch dimensions are kept constant. Using this concept, the patch resonance frequencies can be controlled and adjusted to the desired band. Three new compact circular microstrip antenna configurations have been proposed to verify the concept of patch reconfiguration. The proposed antennas have been designed, analyzed, and simulated using CST Microwave Studio simulator. The three proposed antennas have been fabricated on FR-4 substrate and their parameters have been measured. Good agreement has been obtained between the simulated and the measured values. The proposed antenna configurations have achieved enhanced parameters as compared to the current 4G antennas. The gain is improved by 20% and the radiation efficiency is enhanced by 10%. The operating bandwidth has been widened several of hundreds of megahertz (270–1000). Finally, the presented antenna configurations achieve perfect VSWR (1.1–1.5).

## REFERENCES

1. Abdelaal, M. A. and H. H. M. Ghouz, "Novel compact broadband and dual-band patch antennas," *IEEE International Symposium on Wireless Communication Systems (ISWCS)*, 890–894, 2012.
2. Addaci, R., A. Diallo, C. Luxey, P. L. Thuc, and R. Staraj, "Dual-band WLAN diversity antenna system with high port-to-port isolation," *IEEE Antennas and Wireless Propagation Letters*, Vol. 11, 244–247, 2012.
3. Anguera, J., C. Puente, C. Borja, and J. Soler, "Dual-frequency broadband-stacked microstrip antenna using a reactive loading and a fractal-shaped radiating edge," *IEEE Antennas and Wireless Propagation Letters*, Vol. 6, 309–312, 2007.
4. Azer, M., S. Shams, and A. Allam, "Compact double-sided printed omni-directional ultra wideband antenna," *IEEE 14th International Symposium on Antenna Technology and Electromagnetic, and the American Electromagnetics Conference (ANTEM-AMEREM)*, 1–4, 2010.
5. Choukiker, Y., S. K. Behera, B. K. Pandey, and R. Jyoti, "Optimization of planar antenna for ISM band using PSO," *IEEE Second International Conference on Computing, Communication and Networking Technologies (ICCCNT)*, 1–4, 2010.
6. Gheethan, A. A. and D. E. Anagnostou, "Broadband and dual-band coplanar folded-slot antennas (CFSAs) [antenna designer's notebook]," *IEEE Trans. Antennas Propag. Magazine*, Vol. 53, No. 1, 80–89, 2011.
7. Li, Z. and C. Ruan, "A small integrated bluetooth and UWB antenna with WLAN band-notched characteristic," *IEEE Proceedings of International Symposium on Signals, Systems and Electronics (ISSSE)*, Vol. 1, 1–4, 2010.
8. Lu, J., Z. Kuai, and X. Zhu, "Broadband suspended patch antenna fed by co-planar double L-probes," *2012 IEEE International Workshop Antenna Technology (iWAT)*, 80–83, 2012.
9. Maci, S. and G. Biffi Gentili, "Dual-frequency patch antennas," *IEEE Trans. Antennas Propag. Magazine*, Vol. 39, No. 6, 13–20, Dec. 1997.
10. Mohammadirad, M., N. Komjani, and M. Yazdi, "Design and implementation of a new UWB microstrip antenna," *IEEE 14th International Symposium on Antenna Technology and Electromagnetic, and the American Electromagnetics Conference (ANTEM-AMEREM)*, 1–4, 2010.
11. Swelam, W., M. A. Soliman, and A. Gomaa, "Compact dual-band microstrip patch array antenna for MIMO 4G communication systems," *IEEE Antennas and Propagation Society International Symposium (APSURSI)*, 1–4, 2010.
12. CST Microwave Studio, Version 2011.